Bull. Chem. Soc. Ethiop. **2023**, 37(6), 1369-1382.
DOI: https://dx.doi.org/10.4314/bcse.v37i6.6

ISSN 1011-3924
Printed in Ethiopia
Online ISSN 1726-801X

ADSORPTION OF LEAD(II) IONS USING KOH-ACTIVATED CARBON DERIVED FROM WATER HYACINTH

Asmamaw Taye*, Solomon Mehretie and Shimelis Admassie

Department of Chemistry, Addis Ababa University, P.O. Box 1176, Addis Ababa, Ethiopia

(Received May 18, 2023; Revised July 7, 2023; Accepted August 22, 2023)

ABSTRACT. In this study, the adsorption of Pb(II) ions onto potassium hydroxide activated carbon derived from water hyacinth leaf (KOH-AC-WHL) is described. KOH-AC-WHL was characterized using FT-IR spectrometry. The adsorption kinetics and equilibrium were investigated using square wave anodic striping voltammetry (SWASV) for monitoring Pb(II) ions. The adsorption kinetics showed a better fit with the pseudo-second-order kinetics model with good linear correlation coefficients (R^2) value of 0.999 compared to R^2 value of 0.760 for a pseudo-first-order kinetics. The Langmuir and Freundlich models were used to fit the adsorption experimental data. A better correlation with the Langmuir model was observed with R^2 value of 0.994 compared to the R^2 value of 0.986 for the Freundlich model. Hence, the maximum adsorption capacity of the adsorbent for Pb(II) ions was calculated from the Langmuir isotherm and found to be 206 mg/g. Thermodynamic parameters were determined and their values showed that the adsorption of Pb(II) ions on KOH-AC-WHL was spontaneous and endothermic. The adsorbent material effectively removed Pb(II) ions from 100 µg/L of Pb(II) simulated wastewater to the World Health Organization (WHO) permissible level of 10.0 µg/L within 30 min. The reusable efficiency of KOH-AC-WHL was found to be 73% after four consecutive cycles.

KEY WORDS: Lead(II) ions, Activated carbon, Water hyacinth, Adsorption

INTRODUCTION

With rapid industrialization and a population explosion, releasing large amounts of heavy metals has inevitably caused environmental pollution [1]. Lead is one of the non-biodegradable and persistent toxic metals found in industrial wastes from glass manufacturing, matches, explosives, photographic materials, mining, melting, batteries, ceramics, lead piping, and metal electroplating industries [2]. It can enter and accumulate into human blood via food chain and cause severe effects on the nervous system, lung, kidney, liver, brain, hematopoietic system, reproductive systems, and can also reduce intelligence quotient (IQ) [3]. According to the World Health Organization (WHO) and US Environmental Protection Agency (US EPA) guidelines, the maximum allowable concentration of lead in drinking water is 10 and 15 µg/L, sequentially [4].

Various techniques, such as ion exchange [5], ion floatation [6], chemical precipitation [7], electrochemical reduction [8], solvent extraction [9], membrane filtration [10], and adsorption [11], have been utilized for Pb(II) ions removal from the aqueous environment. However, adsorption is a well-known effective technique for pollutant removal because of its ease of operation, availability of adsorbents, and the possibility of reusing the spent adsorbent [11].

Recently, various bio-adsorbents, clay minerals, zeolites, polymers, metal oxides, and activated carbon, which can serve as adsorption sites for heavy metal ions, have been significantly used for wastewater treatment [12–14]. Among these adsorbents, activated carbon possesses highly developed porosity, internal surface area, high mechanical strength, and high efficiency over a wide concentration range with low secondary pollution with suitable regeneration operation [11].

Several activated carbon-based adsorbents, such as cobalt ferrite-supported activated carbon [15], KOH-activated maize stalk [16], commercial activated carbon [17], coconut shell activated

*Corresponding author. E-mail:asmamawtaye@gmail.com

carbon [18], *Luffa cylindrica* doped chitosan activated carbon [12], hazelnut husk activated carbon[14], *Euphorbia rigida* activated carbon [19], amino-functionalized mesoporous silica, mercapto functionalized mesoporous silica, and carboxylic-functionalized activated carbon [20], *Typha angustifolia* and *Salix matsudana* activated carbon [21], palm oil mill effluent activated carbon [22], pine cone activated carbon [23], and banana peels and cauliflower leaves biochar [24], and lignin from *Hagenia abyssinica* [25] have been successfully used for the removal of lead from aqueous medium. However, most commercially activated carbons are costly and environmentally unfriendly, using non-renewable and expensive source materials as the precursors. Recently, attention has been focused on the use of low-cost and ever-present lingo-cellulosic plant materials to synthesize activated carbons for lead-polluted water treatment [11].

Water hyacinth is a floating recurrent herbaceous plant native to South America Amazon river basin, found throughout the world and introduced to Ethiopia in 1965 [26, 27]. It grows and reproduces quickly, causing navigation jams, interfering with irrigation, fishing, and power generation; blocking sunlight penetration; lowering water dissolved oxygen (DO) concentration; competitively excluding submerged plants; and reducing biological diversity [11]. Activated carbon production from water hyacinth is considered an appropriate technology to obtain efficient adsorbents at low cost, and also has a high surface area and enriched functional groups, with the goal of controlling the water hyacinth invasive weed and solving environmental pollution problems [28, 29].

Various activated carbon from water hyacinth leaf was used for the adsorption of Pb(II), and a lower adsorption capacity was reported [11]. It may need other activation methods and chemicals to enhance the removal efficiency of Pb(II) ions. Hence, KOH-activated carbon from water hyacinth leaf is prepared, and the adsorption capacity of Pb(II) was studied by optimizing various parameters like pH, adsorbent dosage, contact time, and initial Pb(II) ions concentration using batch experiments. The obtained adsorption capacity (206 mg/g) is higher than ever reported using water hyacinth based materials for Pb(II) ions removal. Electrochemical methods, particularly the SWASV techniques, were used to determine Pb(II) ions which has many advantages, such as the inherent miniaturization of an instrument, low power requirements, low cost, high sensitivity, and fast response [30].

EXPERIMENTAL

Apparatuses

CH Instrument Electrochemical Analyzer (CHI840C) was used for SWASV measurements. A three-electrode configuration consisting of a bismuth film modified glassy carbon electrode (BiFGE), and Nafion-coated bismuth film modified glassy carbon electrode (NC-BiFGE) working electrode, silver/silver chloride (Ag/AgCl/KCl (saturated)) reference electrode, and a platinum wire as a counter electrode was employed. All electrochemical experiments were carried out in one-compartment voltammetric cells at room temperature. A magnetic stirrer together with a magnetic bar was used when needed. KS Oscillator was used for batch adsorption experiments. The pH measurements were carried out using a JENWAY 3510 pH meter.

Reagents

Analytical grade reagents like as, $Bi(NO_3)_3.5H_2O$ (Riedel-de Haen) and $Pb(NO_3)_2$ (Wagtech International Ltd. UK), were used as electrode modifiers and analytes, correspondingly. CH_3COONa (BDH Chemicals Ltd, Poole, England) and CH_3COOH (Merck KGaA 64271 Darmstadt, Germany) were used for the preparation of supporting electrolytes. Deionized water was used to prepare all standard solutions throughout the experiment. KOH (Sigma Aldrich) was used for the preparation of activated carbon, and HCl (37%, Fluka, Germany), and NaOH (assay > 97% (RPE, ACS-ISO for analysis), were used to correct the pH of the solution.

Adsorbent preparation

KOH-AC-WHL was prepared according to reference [29] with some modifications. In brief, water hyacinth leaves (WHL) were collected from Lake Tana, Bahir Dar, Ethiopia. The collected leaf material was cut, and cleaned using tap water and deionized water. The cleaned WHL was oven dried at 60 ^{0}C for 24 hours, and ground to a particle size of roughly 200 µm. It was then washed with 1.0 M HCl, dried, and thermally carbonized for 1 hour in high temperature furnace at 500 ^{0}C under nitrogen atmosphere. Following the carbonization, a 4:1 mass ratio of KOH: biochar is ground until it becomes uniform. The mixture was then placed in the furnace for activation at 800 ^{0}C under a nitrogen atmosphere for 1 hour. The recovered KOH-AC-WHL was washed using 1.0 M HCl and double distilled water until it becomes neutral. The neutralized KOH-AC-WHL was dried in a vacuum oven at 60 ^{0}C for 3 hours.

Preparation of bismuth film modified glassy carbon electrode and Nafion-coated bismuth film modified glassy carbon electrode for square wave anodic stripping voltammetry measurements

Bismuth film modified glassy carbon electrode (BiFGE) and Nafion-coated bismuth film modified glassy carbon electrode (NC-BiFGE) were prepared following the procedure reported by our group earlier [25]. Briefly, the BiFGE was prepared by *in situ* potentiostatic method using a three-electrode system in 0.1 M acetate buffer solution (pH 4.5) containing 1 mg/L of Bi(III) ions by applying a potential of −1.2 V for 240 s. NC-BiFGE was prepared similarly after casting 1% Nafion solution and dimethylformamide (5 µL drop each) on the glassy carbon electrode. Before each measurement, the cleaning step was applied by holding the potential of the working electrode at −0.3 V for 30 s. The experiments were carried out at room temperature in non-deaerated solutions.

Adsorption experiments

A 0.1 mM (each) stock solutions of Bi(III) and Pb(II) were prepared using $Bi(NO_3)_3.5H_2O$ and $Pb(NO_3)_2$, respectively, in 0.1 M acetate buffer, which was prepared from CH_3COONa and CH_3COOH using deionized water. Different concentrations of Bi(III) ions and Pb(II) were prepared by diluting from the stock solution.

The adsorption experiments were conducted in an Erlenmeyer flask with a capacity of 50 mL containing 10 mL of aqueous Pb(II) ions solutions of different concentrations and an adsorbent dosage of 1 g/L of KOH-AC-WHL. The solution pH was optimized and maintained at pH 6.0 using 0.1 M HCl, and 0.1 M NaOH. For adsorption kinetic tests, 10 mg of KOH-AC-WHL was added to 10 mL Pb(II) ions solutions (100 mg/L) at a pH of 6.0 for 5-240 min. Equilibrium studies were carried out by shaking Pb(II) solutions of different concentrations (50–800 mg/L) with 1 g/L KOH-AC-WHL for 240 min at pH 6.0. Thereafter, the Pb(II) ions content in the supernatant liquid was measured using the SWASV technique. The adsorption capacity and the percent of removal of Pb(II) were calculated using equations (1) and (2), respectively [11]:

$$q_e = \frac{(C_o - C_e)V}{m} \tag{1}$$

$$\%\,\text{Removal} = \frac{(C_o - C_e)}{C_0} \times 100 \tag{2}$$

where q_e (mg/g) represents the equilibrium adsorption capacity, C_o and C_e indicate the initial and equilibrium concentration of Pb(II) ions respectively, m (g) is the mass of the adsorbent, and V (L) is the volume of the Pb(II) ions solution.

pH of point of zero charge (pH_{PZC}) *measurement*

The pH drift method was applied to measure pH_{PZC} values. This method is less time-consuming, and the results are perfect than the ones obtained from other applied methods such as titrations [31]. Accordingly, solutions of 0.01 M NaCl in 10 mL test tubes were adjusted to pH values of 1.0 to 12.0 using 0.1 M NaOH and 0.1 M HCl. Then, 10 mg of KOH-AC-WHL was added to test tubes containing 10 mL of 0.1 M NaCl solution and shaken at 200 rpm. After 24 hours, the final pH of the samples was measured and plotted against the initial pH. The intersection point of the resulting curve with the line passing its origin gives pH_{PZC}.

Desorption and regeneration experiments

The regeneration studies were conducted according to reference [32]. In brief, 100 mg/L Pb(II) ions concentration, 1.0 g/L adsorbent dosage, the solution pH 6.0, was agitated for 90 min at room temperature. The KOH-AC-WHL, in the recovered solution, was filled with deionized water and shaken for 180 min at a speed of 200 rpm. Then, the sorbent was filtered, and the equilibrium concentration of desorbed ions in an aqueous solution was measured. The process was repeated six times.

RESULTS AND DISCUSSION

Characterization of KOH-AC-WHL

The FTIR spectra of KOH-AC-WHL without and with Pb(II) ions loaded were recorded within 400-4000 cm^{-1} as shown in Figure 1a, and b.

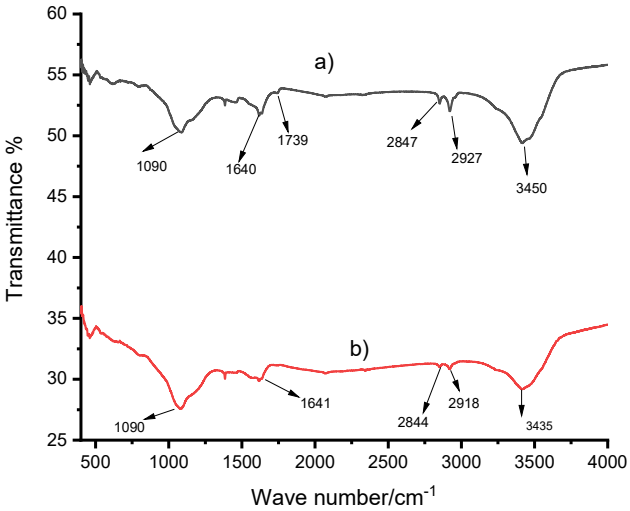

Figure 1. FT-IR spectra of a) KOH-AC-WHL and b) KOH-AC-WHL-Pb(II).

The KOH-AC-WHL presents peak around 3470, 2927, 2847, 1739, 1640, and 1090 cm^{-1} which was attributed to vibration of O–H, sp^3 C-H, sp^2 C-H, C=O, C=C, and C-O functional groups, respectively. The FT-IR spectrum for KOH-AC-WHL-Pb(II) shows the shift, disappearance, and decrease in the intensity of the peaks due to the interaction of Pb(II) ions with hydroxyl and carboxyl functional groups as shown in Figure 1b. This means that the groups were

participating in the adsorption to a certain extent to produce new functional groups as a result of complexation Pb(II) ions with the main functional groups which is in agreement with reference [33].

The SWAS voltammograms and the calibration curves used for monitoring the amount of Pb(II) ions at BiFGE and NC-BiFGE are shown in Figure 2a, and b, respectively.

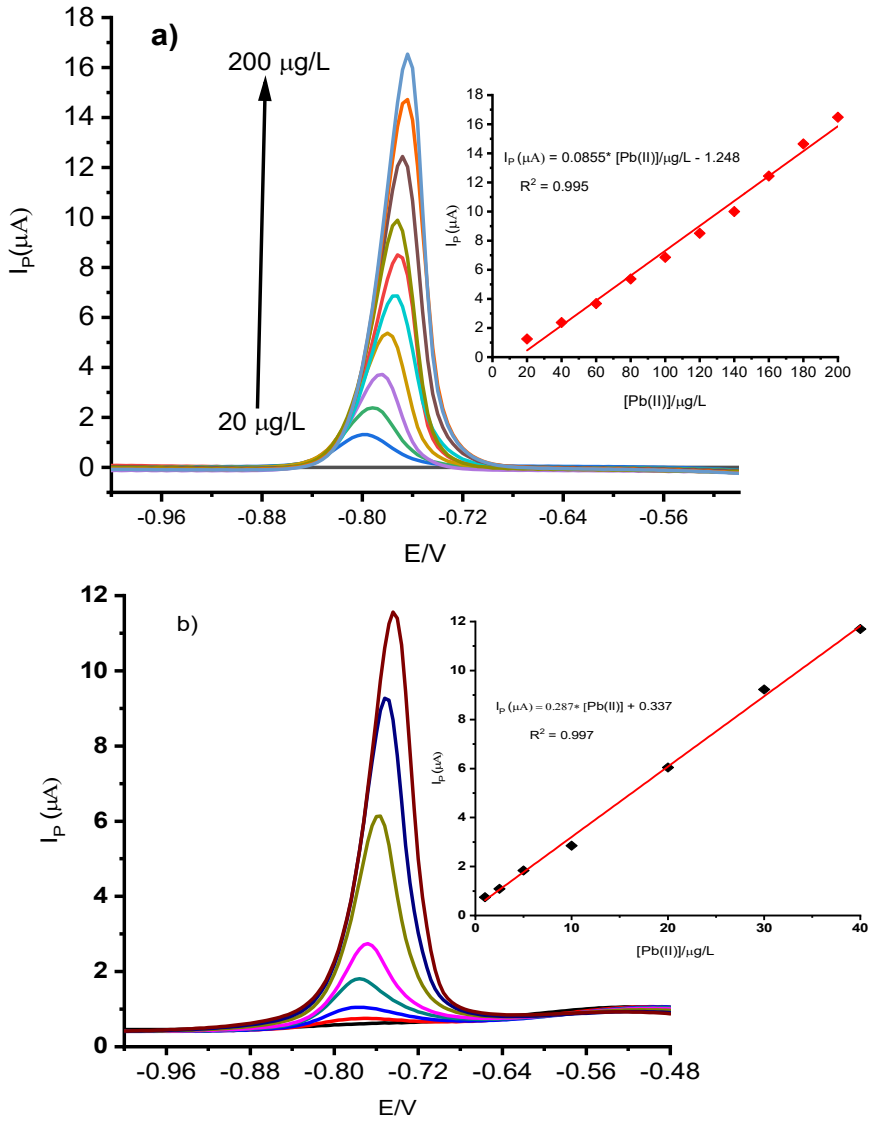

Figure 2. SWAS voltammograms as a function of Pb(II) ions concentration of a) 20–200 µg/L at BiFGE and b) 1.0–40 µg/L at NC-BiFGE in 0.1 M acetate buffer (pH 4.5). Inset: corresponding calibration curves.

The anodic stripping currents were found to be linear as a function of the concentrations of Pb(II) ions in the ranges of 20–200 µg/L and 1.0–40 µg/L at BiFGE and NC-BiFGE, respectively. A linear equation of Ip (µA) = 0.0855*[Pb(II)] – 1.248 with a correlation coefficient of 0.995 was obtained at BiFGE, and Ip (µA) = 0.287*[Pb(II)] + 0.337 with a correlation coefficient of 0.997 was obtained at NC-BiFGE. The limit of detection (LOD) was calculated using Eq. (3):

$$LOD = \frac{3SD}{m} \tag{3}$$

where SD is the standard deviation of the blank solution and m is the slope of the calibration line.

The standard deviation (SD) was calculated by measuring the anodic stripping signals of 10 samples of the blank solution. The detection limit calculated was found to be 0.55 µg/L and 0.21 µg/L at BiFGEand NC-BiFGE, respectively.

The sensitivity for lead ions at NC-BiFGE (0.287 µA L/µg) was found to be three times higher than that of BiFGE (0.0855 µA L/µg). This result can be ascribed to the cation ion exchangeability of Nafion film. The negatively charged sulfonate groups in the Nafion film could facilitate the non-faradaic preconcentration of metal ions [34].

Effect of pH of the solution, adsorbent dosage, contact time, and equilibrium concentration

Figure 3a, b, c, d, e, and f depicts the effect of pH, pH_{PZC}, adsorbent dosage, contact time, equilibrium concentration, and concentration time profile for the adsorption of Pb(II) ions onto KOH-AC-WHL, respectively.

The adsorption capacity increased with increasing pH and reached a maximum at pH 6.0 as shown in Figure 3a. The lower adsorption capacity at lower pH is attributed to the fact that at a low pH, hydrogen ions (H^+) in solution competes with the metal ions. Due to the precipitation of Pb(II) as $Pb(OH)_2$, the adsorption studies were not carried out at pH higher than 6.0. Hence, for further study, pH 6.0 was employed to ensure optimal pH, and it agrees the literature reported in reference [32]. In addition, the pH_{PZC} of KOH-AC-WHL was found to be 1.5 as shown in Figure 3b. Electrostatic repulsion inhibits Pb(II) ions adsorption onto the surface of KOH-AC-WHL at pH < 1.5.With increasing pH, the negatively charged available active sites on the KOH-AC-WHL gradually increased, resulting in a strong electrostatic attraction favouring the adsorption of Pb(II) ions.

The effect of adsorbent dosage on percent removal and adsorption capacity was shown in Figure 3c. Increasing KOH-AC-WHL dosage increases the percent removal while decreasing the adsorption capacity, an effect also reported by others [11]. The increased adsorbent dose provides additional active sites leading to increased percent removal. But, at high adsorbent concentrations, the percent removal reaches a maximum constant value. This is due to the agglomeration of the adsorbent which decreases the unoccupied adsorption active sites and the effective surface area. The initial concentration and volume of Pb(II) ions are constant; the number of ions contacted and adsorbed by the adsorbent per unit mass decreases with the increase in the adsorbent dose, and the active sites of the adsorbents are not saturated. Hence, with the increase in the adsorbent dose, the adsorption capacity of Pb(II) gradually decreases, and similar results are reported in reference [35].

The experimental data relating to the adsorption processing time of the Pb(II) ions is illustrated in Figure 3d.The adsorption capacity was observed to increase rapidly at the initial stages of the sorption process and gradually decrease at around 90 min. The purpose of this could be linked to the fact that the adsorbent at the initial stage possesses an incredibly large volume and pores available for the adsorption or ion uptakes. The adsorption of Pb(II) ions was fast for up to 60 min, and thereafter they gradually reached equilibrium at 90 min. Maximum sorption was obtained at 90 min, with Pb(II) ions showing an adsorption capacity of 62.5 mg/g. Moreover, a further increase in contact time had no significant influence on the adsorption capacity of the

metal ion, probably due to the saturation of the adsorbent surface with Pb(II) ions which is in agreement with reference [15]. Therefore, the optimum contact time was chosen as 90 min for the process and further investigation.

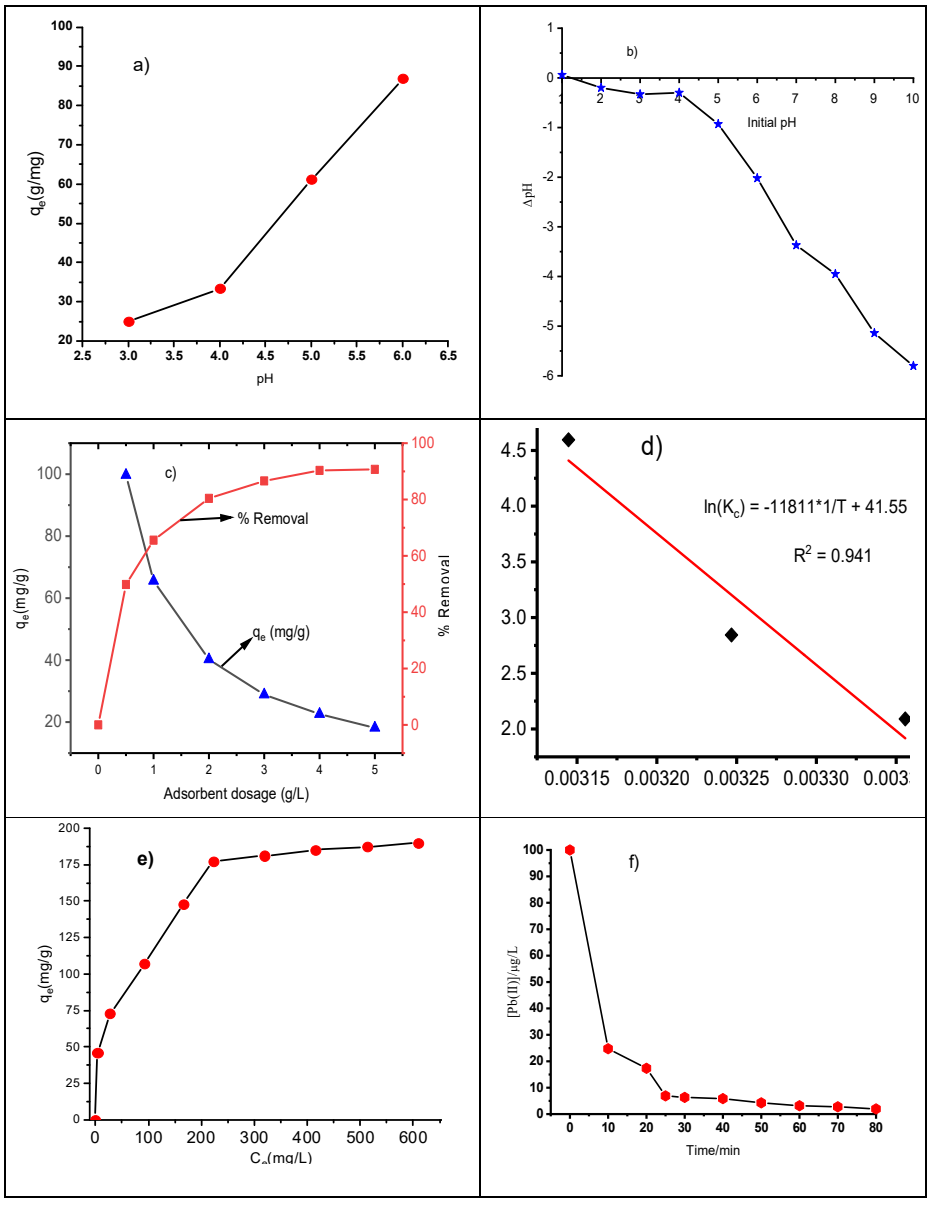

Figure 3. The effect of; a) pH of the solution, b) pH_{PZC}, c) adsorbent dosage, d) contact time, e) equilibrium concentration of Pb(II) ions using KOH-AC-WHL. ([Pb(II)], 100 mg/L), and f) concentration-time profile for removal of 100 μg/L of Pb(II) ions.

The adsorption of Pb(II) ions increased when the equilibrium concentration (Ce) was lower than 250 mg/L, as shown in Figure 3e. All active available surface sites were partially saturated when the Pb(II) concentration was greater than 250 mg/L, indicating their restricted accessibility with the increase in the amounts and concentrations of Pb(II) [36]. It was also found that 100 µg/L of Pb(II) ions is reduced to the WHO permissible level of 10 µg/L within about 30 min using KOH-AC-WHL (Figure 3f).

Adsorption isotherm, kinetics and thermodynamic studies

The graphical representations of Langmuir and Freundlich models, the pseudo-first-order and pseudo-second-order kinetics, and adsorption thermodynamics are presented in Figure 4a, b, c, and d, respectively.

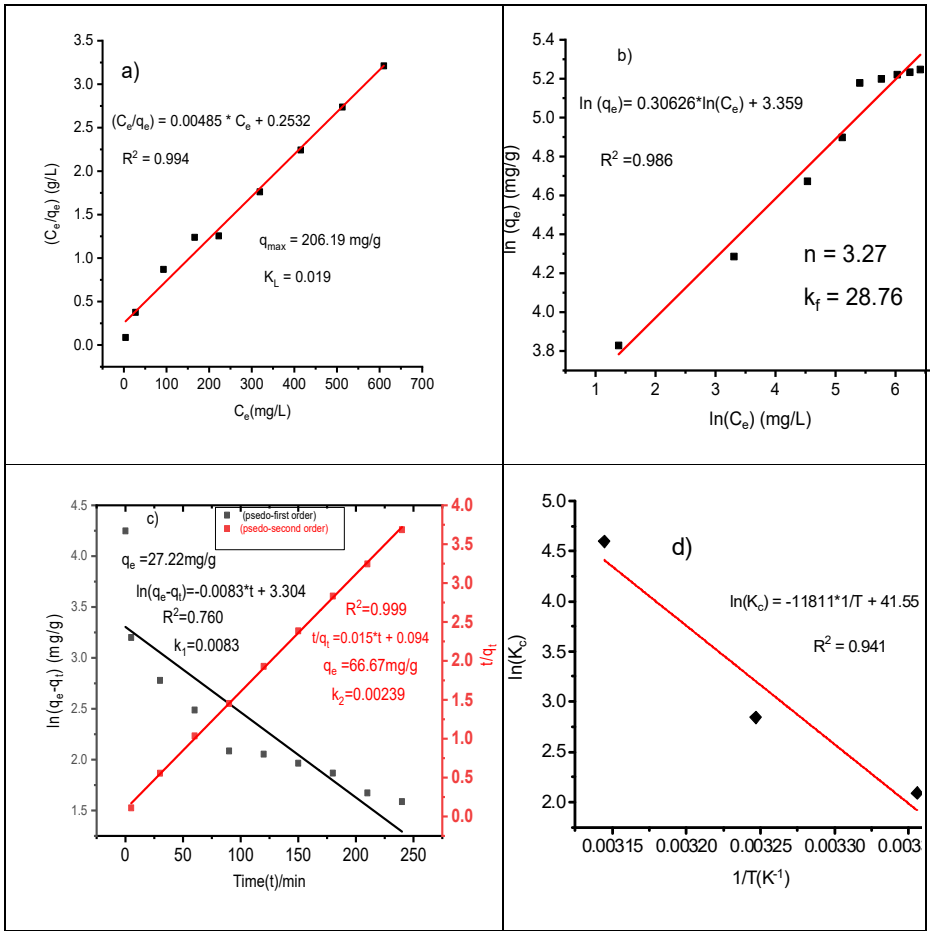

Figure 4. Linear model fitting of a) Langmuir, b) Freundlich isotherm; c) pseudo-first order and pseudo-second order kinetic fitting, and d) thermodynamic parameters.

The adsorption isotherms were analyzed by linear fitting into the Langmuir and Freundlich models using equations (4) and (5) respectively [26]:

$$\frac{C_e}{q_e} = \frac{1}{K_L q_{\max}} + \frac{C_e}{q_{\max}} \tag{4}$$

$$\ln(q_e) = \ln(K_F) + \frac{1}{n}\ln(C_e) \tag{5}$$

where q_e (mg/g) is the equilibrium adsorption capacity, C_e (mg/L) is the equilibrium concentration, K_L (L/mg) is the Langmuir adsorption constant, q_{max} (mg/g) is the maximum adsorption capacity, K_F is the Freundlich constant, 1/n is the heterogeneity factor. The parameters obtained from the linear fitting of Langmuir and Freundlich models provide important information on the affinity of the adsorbent, the sorption mechanisms, and the surface properties of the adsorbent. The Langmuir model gave the most accurate estimations R^2 0.994 indicating that, a homogenous adsorption rate, with equal adsorbent affinity, with single-layer adsorption [37]. Maximum adsorption capacities obtained from the Langmuir model were 206 mg/g

The kinetic behaviour was studied by fitting into the pseudo-first-order and pseudo-second-order equations as shown in equations (6) and (7), respectively [38]:

$$\ln(q_e - q_t) = \ln q_e - k_1 t \tag{6}$$

$$\frac{t}{q_t} = \frac{1}{k_2 q_e^2} + \frac{1}{q_e} \times t \tag{7}$$

where q_t (mg/g) is the amount of adsorbate adsorbed at time t (min), k_1 and k_2 are the rate constants of pseudo-first-order and pseudo-second-order kinetic models, respectively. The pseudo-first-order and pseudo-second-order models in Figure 4c shows, a good fitting to the experimental data with R^2 0.760 and 0.999 for Pb(II) ions, respectively. Moreover, the theoretically calculated adsorption capacities from pseudo-first-order and pseudo-second-order models were found to be 27.22 and 66.67 mg/g, respectively, and the adsorption capacity obtained from the pseudo-second-order model is close to the experimental value. Hence, the pseudo-second-order model can be applied to predict the adsorption kinetics, and so that, the rate-controlling step was chemisorption [39].

The thermodynamic parameters for the adsorption process were calculated by using equations (8), (9) and (10) [13]:

$$\Delta G = -RT \ln Kc \tag{8}$$

$$Kc = \frac{C_A}{C_S} \tag{9}$$

$$\ln Kc = \frac{-\Delta H}{RT} + \frac{\Delta S}{R} \tag{10}$$

where R (8.314 J mol^{-1} K^{-1}) is the gas constant, K_c is the equilibrium constant, T (K) is the temperature, C_A and C_S (mg/L) are the equilibrium concentrations of Pb(II) on the adsorbent, and in the solution, respectively, ΔH is standard enthalpy, and ΔS is the entropy of the adsorption system.

Adsorption thermodynamics can help to understand the nature of the adsorption process. It was observed that the adsorption capacities increased from 130 to 175 mg/g as the temperature was increased from 298 to 318 K which indicates a chemical interactions between the adsorbate and adsorbent. Furthermore, the ΔG increased from -5.179 to -12.16 kJ/mol when the adsorption temperature increased from 298 to 318 K, indicating favourable adsorption at higher temperature The ΔH and ΔS values were calculated as 98.20 kJ/mol and 0.345 kJ/mol K, respectively, from a plot of ln (Kc) vs 1/T. The positive value of ΔH indicates that the adsorption of Pb(II) ions is endothermic. The positive value of ΔS tells that the randomness increases at the interface between Pb(II) ions and the surface of KOH-AC-WHL during the adsorption process and it is in agreement with literature [40].

Reusability study

The reusing efficiency of KOH-AC-WHL for four consecutive cycles is shown in Figure 5.The reusability of the adsorbents is important for the economic feasibility and practical implications. The reuse efficiency of KOH-AC-WHL decreases up to 73% in the first four desorption recycling experiments. As supported from literature [36], it can be generalized that KOH-AC-WHL is suitable for the re-adsorption of heavy metals from wastewater.

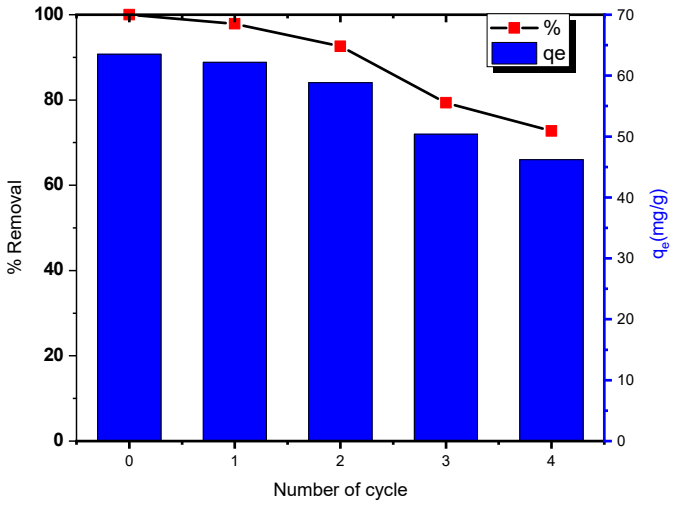

Figure 5. KOH-AC-WHL recycling study (pH 6.0; contact time 90 min; [Pb(II)]; 100 mg/L).

The maximum adsorption capacities of different adsorbents for Pb(II) ions adsorption were compared with similar adsorbent materials reported in the literature in Table 1.

The adsorption capacity of KOH-AC-WHL was higher than most of the adsorbents listed in Table 1 except for that of *Luffa cylindrica* doped chitosan-activated carbon adsorbent, indicating that the prepared material improves the adsorption capacity of some other similar adsorbents. Accordingly, KOH-AC-WHL is a promising adsorbent for the removal of Pb(II) ions from aqueous solutions due to the possibility of scalability and modification of KOH-AC-WHL to enhance the adsorption capacity more than the reported value.

Table 1.Comparison of Pb(II) ions adsorption capacity of different adsorbents.

Types of adsorbent	q_{max} (mg/g)	References
Water hyacinth powder	75.44	[41]
H_3PO_4 activated water hyacinth carbons	118.8	[11]
Cobalt ferrite-supported activated carbon	6.27	[15]
KOH-activated maize stalk	206	[16]
Commercial activated carbon	9.30	[17]
Coconut shell-activated carbon	29.44	[18]
Luffa cylindrica doped chitosan-activated carbon	279.7	[12]
Typha angustifolia and *Salix matsudana* activated carbon	61.33 and 58.82	[21]
Palm oil mill effluent activated carbon	69.44	[22]
Pine cone-activated carbon	27.53	[23]
Banana peels and cauliflower leaves biochar	75.99 and 53.96	[24]
Lignin from *Hagenia abyssinica*	80.05	[25]
KOH-AC-WHL	206.2	This work

CONCLUSION

The present investigation shows that KOH-AC-WHL is an effective adsorbent for the removal of Pb(II) ions from an aqueous solution. The removal of Pb(II) ions using KOH-AC-WHL was pH-dependent and better adsorption capacity was obtained at pH 6.0, a contact time of 90 min, at an optimum dose of 1 g/L, suggesting that this is a reasonable and cost-effective adsorption technique. The experimental adsorption data were fitted to Langmuir and Freundlich isotherm models. Experimental results are in good agreement with the Langmuir adsorption isotherm model, with a maximum monolayer adsorption capacity of 206 mg/L. The cost of Pb(II) ions removal using KOH-AC-WHL is quite low as the raw materials for the synthesized adsorbent are easily available in large amounts from highly invasive weeds. Moreover, this is a simple technique to control the spread of unwanted water hyacinth weed by utilization.

ACKNOWLEDGMENTS

The financial support from the Ethiopian Biotechnology Institute and the International Science Program (ISP), Uppsala University, Sweden is greatly acknowledged.

REFERENCES

1. Wang, P.; Tang, Y.; Liu, Y.; Wang, T.; Wu, P.; Lu, X.-Y. Halloysite nanotube@carbon with rich carboxyl groups as a multifunctional adsorbent for the efficient removal of cationic Pb(II), anionic Cr(VI) and methylene blue (MB). *Environ. Sci. Nano* **2018**, 5, 2257–2268.
2. Singh, N.; Kumar, A.; Gupta, V.K.; Sharma, B. Biochemical and molecular bases of lead-induced toxicity in mammalian systems and possible mitigations. *Chem. Res. Toxicol.* **2018**, 31, 1009–1021.
3. Huang, K.; Li, B.; Zhou, F.; Mei, S.; Zhou, Y.; Jing, T. Selective solid-phase extraction of lead ions in water samples using three-dimensional ion-imprinted polymers. *Anal. Chem.* **2016**, 88, 6820–6826.
4. Chowdhury, I.R.; Chowdhury, S.; Mazumder, M.A.J.; Al-Ahmed, A. Removal of lead ions (Pb^{2+}) from water and wastewater: A review on the low-cost adsorbents. *Appl. Water Sci.* **2022**, 12), 185.

5. Lalmi, A.; Bouhidel, K.-E.; Sahraoui, B.; Anfif, C.E.H. Removal of lead from polluted waters using ion exchange resin with $Ca(NO_3)_2$ for elution. *Hydrometallurgy* **2018**, 178, 287–293.
6. Yuan, X.Z.; Meng, Y.T.; Zeng, G.M.; Fang, Y.Y.; Shi, J.G. Evaluation of tea-derived biosurfactant on removing heavy metal ions from dilute wastewater by ion flotation. *Colloids Surf. A Physicochem. Eng. Asp.* **2008**, 317, 256–261.
7. Aziz, H.A.; Adlan, M.N.; Ariffin, K.S. Heavy metals (Cd, Pb, Zn, Ni, Cu and Cr(III)) removal from water in Malaysia: Post treatment by high quality limestone. *Bioresour. Technol.* **2008**, 99, 1578–1583.
8. Liu, Y.; Yan, J.; Yuan, D.; Li, Q.; Wu, X. The study of lead removal from aqueous solution using an electrochemical method with a stainless steel net electrode coated with single wall carbon nanotubes. *Chem. Eng. J.* **2013**, 218, 81–88.
9. Shah, D.B.; Phadke, A.V.; Kocher, W.M. Lead removal from foundry waste by solvent extraction. *J. Air Waste Manag. Assoc.* **1995**, 45, 150–155.
10. Yang, R.; Aubrecht, K.B.; Ma, H.; Wang, R.; Grubbs, R.B.; Hsiao, B.S.; Chu, B. Thiol-modified cellulose nanofibrous composite membranes for chromium(VI) and lead(II) adsorption. *Polymer* **2014**, 55, 1167–1176.
11. Huang, Y.; Li, S.; Chen, J.; Zhang, X.; Chen, Y. Adsorption of Pb(II) on mesoporous activated carbons fabricated from water hyacinth using H_3PO_4 activation: adsorption capacity, kinetic and isotherm studies. *Appl. Surf. Sci.* **2014**, 293, 160–168.
12. Gedam, A.H.; Dongre, R.S. Activated carbon from *Luffa cylindrica* doped chitosan for mitigation of lead(II) from an aqueous solution. *RSC Adv.* **2016**, 6, 22639–22652.
13. Largitte, L.; Brudey, T.; Tant, T.; Dumesnil, P. C.; Lodewyckx, P. Comparison of the adsorption of lead by activated carbons from three lignocellulosic precursors. *Micropor. Mesopor. Mater.* **2016**, 219, 265–275.
14. Imamoglu, M.; Tekir, O. Removal of copper(II) and lead(II) ions from aqueous solutions by adsorption on activated carbon from a new precursor hazelnut husks. *Desalination* **2008**, 228, 108–113.
15. Yahya, M.D.; Obayomi, K.S.; Abdulkadir, M.B.; Iyaka, Y.A.; Olugbenga, A.G. Characterization of cobalt ferrite-supported activated carbon for removal of chromium and lead ions from tannery wastewater via adsorption equilibrium. *Water Sci. Eng.* **2020**, 13, 202–213.
16. El-Hendawy, A.-N.A. An insight into the KOH activation mechanism through the production of microporous activated carbon for the removal of Pb^{2+} cations. *Appl. Surf. Sci.* **2009**, 255, 3723–3730.
17. Kavand, M.; Eslami, P.; Razeh, L. The adsorption of cadmium and lead ions from the synthesis wastewater with the activated carbon: Optimization of the single and binary systems. *J. Water Process Eng.* **2020**, 34, 101151.
18. Goel, J.; Kadirvelu, K.; Rajagopal, C.; Kumar Garg, V. Removal of lead(II) by adsorption using treated granular activated carbon: Batch and column studies. *J. Hazard. Mater.* **2005**, 125, 211–220.
19. Gerçel, Ö.; Gerçel, H.F. Adsorption of lead(II) ions from aqueous solutions by activated carbon prepared from biomass plant material of *Euphorbia rigida*. *Chem. Eng. J.* **2007**, 132, 289–297.
20. Machida, M.; Fotoohi, B.; Amamo, Y.; Mercier, L. Cadmium(II) and lead(II) adsorption onto hetero-atom functional mesoporous silica and activated carbon. *Appl. Surf. Sci.* **2012**, 258, 7389–7394.
21. Tang, C.; Shu, Y.; Zhang, R.; Li, X.; Song, J.; Li, B.; Zhang, Y.; Ou, D. Comparison of the removal and adsorption mechanisms of cadmium and lead from aqueous solution by activated carbons prepared from *Typha angustifolia* and *Salix matsudana*. *RSC Adv.* **2017**, 7, 16092–16103.

22. Adebisi, G.A.; Chowdhury, Z.Z.; Alaba, P.A. Equilibrium, kinetic, and thermodynamic studies of lead ion and zinc ion adsorption from aqueous solution onto activated carbon prepared from palm oil mill effluent. *J. Clean. Prod.* **2017**, 148, 958–968.
23. Momčilović, M.; Purenović, M.; Bojić, A.; Zarubica, A.; Ranđelović, M. Removal of lead(II) ions from aqueous solutions by adsorption onto pine cone activated carbon. *Desalination* **2011**, 276, 53–59.
24. Ahmad, Z.; Gao, B.; Mosa, A.; Yu, H.; Yin, X.; Bashir, A.; Ghoveisi, H.; Wang, S. Removal of Cu(II), Cd(II) and Pb(II) ions from aqueous solutions by biochars derived from potassium-rich biomass. *J. Clean. Prod.* **2018**, 180, 437–449.
25. Tesfaw, B.; Chekol, F.; Mehretie, S.; Admassie, S. Adsorption of Pb(II) ions from aqueous solution using lignin from *Hagenia abyssinica*. *Bull. Chem. Soc. Ethiop.* **2017**, 30, 473.
26. Zhou, R.; Zhang, M.; Li, J.; Zhao, W. Optimization of preparation conditions for biochar derived from water hyacinth by using response surface methodology (RSM) and its application in Pb^{2+} removal. *J. Environ. Chem. Eng.* **2020**, 8, 104198.
27. Dersseh, M.G.; Tilahun, S.A.; Worqlul, A.W.; Moges, M.A.; Abebe, W.B.; Mhiret, D.A.; Melesse, A.M. Spatial and temporal dynamics of water hyacinth and its linkage with lake-level fluctuation: Lake Tana, a sub-humid region of the Ethiopian highlands. *Water* **2020**, 12, 1435.
28. Zhou, R.; Zhang, M.; Li, J.; Zhao, W. Optimization of preparation conditions for biochar derived from water hyacinth by using response surface methodology (RSM) and its application in Pb^{2+} removal. *J. Environ. Chem. Eng.* **2020**, 8, 104198.
29. Shell, K.M.; Vohra, S.Y.; Rodene, D.D.; Gupta, R.B. Phytoremediation of nickel via water hyacinth for biocarbon-derived super capacitor applications. *Energy Technol.* **2021**, 9, 2100130.
30. Zhang, X.; Zhang, Y.; Ding, D.; Zhao, J.; Liu, J.; Yang, W.; Qu, K. On-site determination of Pb^{2+} and Cd^{2+} in seawater by double stripping voltammetry with bismuth-modified working electrodes. *Microchem. J.* **2016**, 126, 280–286.
31. Pashai Gatabi, M.; Milani Moghaddam, H.; Ghorbani, M. Point of zero charge of maghemite decorated multiwalled carbon nanotubes fabricated by chemical precipitation method. *J. Mol. Liq.* **2016**, 216, 117–125.
32. Neskoromnaya, E.A.; Khamizov, R.K.; Melezhyk, A.V.; Memetova, A.E.; Mkrtchan, E.S.; Babkin, A.V. Adsorption of lead ions (Pb^{2+}) from wastewater using effective nanocomposite GO/CMC/FeNPs: Kinetic, isotherm, and desorption studies. *Colloids Surf. A Physicochem. Eng. Asp.* **2022**, 655, 130224.
33. İrdemez, Ş.; Yeşilyurt, D.; Ekmekyapar Torun, F.; Kul, S. Determination of parameters affecting kinetic and thermodynamic values for lead removal using wastewater treatment plant sewage sludge ash. *Bull. Chem. Soc. Ethiop.* **2022**, 36, 935–948.
34. Xu, H.; Zeng, L.; Huang, D.; Xian, Y.; Jin, L. A Nafion-coated bismuth film electrode for the determination of heavy metals in vegetable using differential pulse anodic stripping voltammetry: An alternative to mercury-based electrodes. *Food Chem.* **2008**, 109, 834–839.
35. Lei, T.; Li, S.-J.; Jiang, F.; Ren, Z.-X.; Wang, L.-L.; Yang, X.-J.; Tang, L.-H.; Wang, S.-X. Adsorption of cadmium ions from an aqueous solution on a highly stable dopamine-modified magnetic nano-adsorbent. *Nanoscale Res. Lett.* **2019**, 14, 352.
36. Ahmed, W.; Mehmood, S.; Núñez-Delgado, A.; Ali, S.; Qaswar, M.; Shakoor, A.; Mahmood, M.; Chen, D.-Y. Enhanced adsorption of aqueous Pb(II) by modified biochar produced through pyrolysis of watermelon seeds. *Sci. Total Environ.* **2021**, 784, 147136.
37. Li, M.; Liu, H.; Chen, T.; Dong, C.; Sun, Y. Synthesis of magnetic biochar composites for enhanced uranium(VI) adsorption. *Sci. Total Environ.* **2019**, 651, 1020–1028.
38. Zhao, J.; Yu, L.; Ma, H.; Zhou, F.; Yang, K.; Wu, G. Corn stalk-based activated carbon synthesized by a novel activation method for high-performance adsorption of hexavalent chromium in aqueous solutions. *J. Colloid Interface Sci.* **2020**, 578, 650–659.

39. Zhou, Q.; Liao, B.; Lin, L.; Qiu, W.; Song, Z. Adsorption of Cu(II) and Cd(II) from aqueous solutions by ferromanganese binary oxide–biochar composites. *Sci. Total Environ.* **2018**, 615, 115–122.
40. Lingamdinne, L.P.; Choi, Y.-L.; Kim, I.-S.; Yang, J.-K.; Koduru, J.R.; Chang, Y.-Y. Preparation and characterization of porous reduced graphene oxide based inverse spinel nickel ferrite nanocomposite for adsorption removal of radionuclides. *J. Hazard. Mater.* **2017**, 326, 145–156.
41. Yi, Z.; Liu, J.; Liu, X.; Zeng, R.; Cui, Y. Lead(II) removal from wastewater by water hyacinth. *IOP Conf. Ser. Earth Environ. Sci.* **2019**, 310, 042015.